RESEARCH PAPER

# Development and Characterization of Isatin Derivatives with Potential Antibacterial Properties

**Sudhir Kumar[1], Azhar Iqbal[2], Nazli Shahin[3], Swamita Arora[4], Mukul Singh[5], Robin Singh[4], Mohammad Rashid[4], Sanjar Alam[4*]**

*[1]IIMT College of Pharmacy, Greater Noida, Uttar Pradesh, India*
*[2]Jamia Hamdard, New Delhi, India*
*[3]Scientific Writer, Dubai*
*[4]R.V. Northland Institute, Dadri, Greater Noida, Uttar Pradesh, India*
*[5]GNIT College of Pharmacy, Greater Noida, Uttar Pradesh, India*
***Corresponding author: sanjaralam10@gmail.com***

***Received: 8 July 2026; Revised: 2 August 2026; Accepted: 15 August 2026; Available Online: 26 August 2026***

**ABSTRACT**

A series of novel 5-bromo isatin derivatives were synthesized through a one-step reaction of 5-bromoisatin with phenylsulfonyl chloride derivatives, yielding compounds SA01 (5-bromo-1-((4-chlorophenyl)sulfonyl)indoline-2,3-dione), SA02 (5-bromo-1-((4-bromophenyl)sulfonyl)indoline-2,3-dione), and SA03 (5-bromo-1-((4-fluorophenyl)sulfonyl)indoline-2,3-dione). Their structures were validated using $^{13}$C-NMR, $^{1}$H-NMR and mass spectroscopy with spectral data consistent with the proposed structures. All derivatives were obtained in high yields (95–98%) and exhibited distinct physical characteristics. The compounds antibacterial action was evaluated against Gram-positive (*Staphylococcus aureus, Bacillus subtilis*) and Gram-negative (*Escherichia coli, Pseudomonas putida*) bacterial strains. Among the examined analogues, SA02 exhibited the strongest antibacterial effect, showing minimum inhibitory concentration (MIC) ranges between 3.12 and 6.14 µg/ml, followed by SA01 (4.12–6.24 µg/ml) and SA03 (4.98–7.14 µg/ml). Although, the compounds were less active than standard antibiotics (amoxicillin and ciprofloxacin), their activity was superior to many previously reported isatin derivatives, emphasizing the role of halogen substitution on the phenylsulfonyl moiety in enhancing antibacterial potency. These findings highlight sulfonyl-isatin hybrids as promising lead scaffolds for further structural optimization towards the development of new antibacterial agents.

**Keywords:** Isatin; 5-Bromoisatin; Antibacterial action; Gram-positive bacteria; Minimum inhibitory concentration

**How to cite this article:** Sudhir Kumar1 Azhar Iqbal2 Nazli Shahin3 Swamita Arora4 Mukul Singh5 Robin Singh4 Mohammad Rashid4 Sanjar Alam4*. Development and Characterization of Isatin Derivatives with Potential Antibacterial Properties. Int J Drug Deliv Technol. 2026;16(78s):1126-1130. DOI: 10.25258/ijddt.16.78s.160.

## 1. Introduction

The ever-increasing prevalence of resistant-germs to antibiotics poses a huge challenge to the health of people all over the world. As a result, it is very necessary to find out new antimicrobial treatments that are both effective and potent. Although antibiotics have revolutionized modern medicine, their overuse and misuse have led to the reduced effectiveness of existing treatments (1, 2). The discovery of antibiotics has undoubtedly marked a major breakthrough in medical science. However, the growing issue of antimicrobial resistance has significantly limited their long-term effectiveness. This challenge underscores the urgent need to develop novel and more potent antibacterial agents or enhance the efficacy of existing ones. In this context, the isatin scaffold has gained considerable attention (3, 4). Isatin**,** first identified as a natural constituent of coal tar, has garnered significant attention in pharmaceutical chemistry due to its diverse pharmacological properties. Endogenously, isatin and related indole derivatives have been detected in mammalian biological fluids such as urine, blood, and adrenal glands, as well as in various plant species, including *Isatis tinctoria*, *Couroupita guianensis*, and *Calanthe discolour*. Additionally, isatin is secreted by the Bufo frog**,** further highlighting its natural abundance and biological relevance (5, 6). Isatin and its derivatives are demonstrated for antimicrobial (antibacterial, antiviral, antifungal) (7)**,** antioxidant (8)**,** anti-inflammatory (9)**,** antitubercular (10)**,** anticancer (11)**,** anticonvulsant (12)**,** anti-HIV (13)**,** anti-coronavirus (14) and anti-hepatitis C effects (15). These therapeutic attributes, combined with their synthetic versatility, make isatin a valuable core for drug design and development (16).

From a structural perspective, Isatin comprises an indole fused-ring system with 2-carbonyl groups at the 2nd - 3rd positions and a nitrogen atom at the 1st position**.** This arrangement allows for extensive chemical modification**,** particularly at the N-1, C-3, C-5 positions**,** enabling development of a wide variety of bioactive analogues. Modifications such as N-alkylation**,** halogenation at the 5-position (with substituents like Br, Cl, and F), and aromatic or heteroaromatic substitution at the 3-position have shown enhanced antibacterial and other therapeutic effects (17, 18). The proposed compound has been rationally designed by integrating structural motifs from previously reported bioactive scaffolds. Isatin and its derivatives, such as semaxanib and indirubin, are well-known pharmacophores with significant therapeutic potential, and some of them have progressed to clinical evaluation or regulatory approval. Semaxanib (SU5416), for example, is a potent tyrosine kinase inhibitor with anticancer activity, while indirubin, an isatin derivative, has been extensively investigated for its role in

modulating kinases involved in cell cycle regulation and cancer progression. On the other hand, phenylsulfonamide derivatives are widely recognized for their diverse biological activities. Classical examples include 4-aminobenzenesulfonic acid and benzenesulfonamide, which are reported for their antibacterial effects and serve as structural frameworks for several sulfonamide-based therapeutic agents. The sulfonamide group is particularly valuable in design an ability for better aqueous solubility, binding interactions, and metabolic stability.

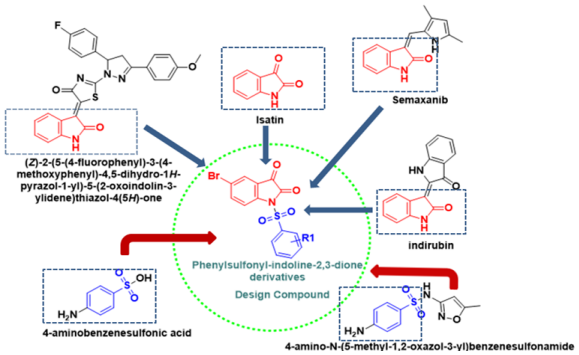


Here, we report to develop novel Isatin derivatives. It is developed and characterised followed by an seeing their pharmacological activities. Our aim is to explore the structure-activity relationship and identify candidates with promising potential as future antimicrobial agents.

## 2. Materials and Methods

### 2.1. General

All solvents and reagents are bought from Sigma-Aldrich Pvt. Ltd. No any further purification was done before uses. 5-bromoisatin was purchased from Merck with catalogue no: 476994, Phenylsulfonyl chloride from Sigma-Aldrich Pvt. Ltd with catalogue no: 6461785, dichloromethane from Sigma-Aldrich Pvt. Ltd with catalogue no: 75-09-2. The synthesis steps reactions regularly and routinely scanned by thin-layer chromatography (TLC) employing suitable systems like petroleum ether:ethyl acetate mixtures. The final compounds were elucidated and confirmed with the chemical structures, through a spectroscopic technique.

For the $^{1}$H- and $^{13}$C-NMR- a JEOL-SPM at 600-M.Hz and 151-M.Hz using DMSO-$d_6$ solvent. Tetramethylsilane (TMS) standard used for chemical shifts (δ) in ppm. Signal used as s (singlet) and d (doublet), with coupling constants (J) in Hz. The spectra for characteristic functional groups, obtained using KBr pellets of compound in Bruker FT-IR. Mass spectra were recorded of drug-in-organic solvents employing standard techniques for structural verification.

### 2.2. Synthetic Design and Development of Isatin-Based Scaffolds

#### 2.2.1. Chemical-Synthesis

The target compounds were synthesized through a one-pot reaction (Figure 2). Phenylsulfonyl chloride derivatives (1 mmol) and 5-bromoisatin (1 mmol) taken to dissolve in DCM in glass container (round-bottom flask). Triethylamine ($(Et)_3$ N, 3–5 mL) poured in the above flask. The addition was dropwise and under constant stirring, side by side reaction temperature at 0–3 °C was maintained on ice bath. The reaction time taken 8–10 h. The thin-layer chromatography (TLC) was used for reaction competion monitoring. TLC solvent taken petroleum-ether/ethyl acetate (1:1). Upon completion, the mixture was quenched and subjected to liquid–liquid extraction (water-ethyl acetate) system. Out of this, organic layer taken in rotary evaporator, to evaporate the solvent under reduced pressure. It afforded the Isatin derivatives (phenylsulfonyl-indoline-2,3-diones) as solid products (20, 21, 22).

In the proposed compound, the Isatin core has been strategically merged with the phenylsulfonamide moiety to yield a hybrid framework that is expected to harness the pharmacological advantages of both scaffolds. This molecular hybridization approach aims to combine the kinase inhibitory potential of isatin derivatives with the antimicrobial and drug-like features of sulfonamides, thereby producing a multifunctional molecule with enhanced bioactivity (19). The structural design of this compound is illustrated in Figure 1, which depicts the fusion of the isatin nucleus with the phenyl ring to generate the novel hybrid scaffold.

**Figure 1: Rational design of the proposed isatin derivative.**

#### 2.2.2. Antimicrobial Profiling (Assay):

The MIC of synthesized molecules against Bacteria was evaluated by the broth dilution method. Here both Gram-positive and Gram-negative bacteria was taken for evaluation. Using the direct colony suspension method, bacterial suspensions in saline was generated with a concentration of $1.5 \times 10^8$ CFU/ml. Through the microdilution approach, the MIC of AgNPs and AuNPs, along with the methanol extract, was evaluated. AgNPs, AuNPs, and extract at several concentrations (0.78 to 50 µg/mL) were formed by two-fold dilutions and added to Muller Hinton broth containing $10^8$ bacterial suspensions. The incubation of mixture was 37° C for a whole day. To determine the minimum amount of drug and extract (MIC) to obstruct 90% of growth, the turbidity of the sample was used to calculate the MIC (23).

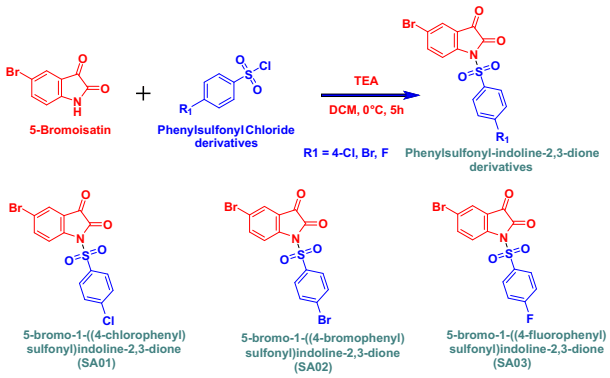


**Figure 2. Schematic representation of the synthesis of Isatin derivatives.**

### 2.2.3. Growth-Inhibition Zone Assay

The antimicrobial efficacy of the test compounds (SA1, SA2 and SA3) was seen in the agar well diffusion method. Serial dilutions (1-16 µg/mL) were taken from a stock (100 µg/mL in dimethyl sulfoxide (DMSO). Bacterial lawns were prepared by swabbing standardized inoculum onto LB agar plates. After dispensing the test solutions into wells, it was kept at 37°C for total 24 h. To enhance visibility ZOI were stained with 1% methylene blue, and their diameters were measured and compared to the standard (amoxicillin and ciprofloxacin) (24).

### 2.2.4. *In vitro antioxidant Profiling of the Test Samples*

2,2-diphenyl-1-picrylhydrazyl (DPPH), ascorbic acid (L-AA), and DMSO of high purity were taken. AR-grade solvents for the preparation of dilutions were taken. Absorbance was recorded on a UV-visible spectrophotometer at a *517 nm* wavelength.

*Preparation of DPPH solution*: 4 mg of it added in solvent 100 ml for getting conc 0.101 mM DPPH stock solution. The freshly prepared dilutions from stock solution with the solvent taken so as produce the absorbance < 1.00 at defined wavelength.

*Preparation of standard and test samples:* Stock solutions of the standard and test compounds (100 mM) were obtained in methanol containing 1% DMSO. These solutions were then diluted serial wise to get working concentrations of 10, 5, 2.5, and 1 mM. After mixing with the DPPH reagent, the final antioxidant concentrations in the reaction mixture were 100, 50, 25, and 10 µM. This range was selected to ensure that the concentrations spanned from well above the DPPH level—minimizing potential diffusion-related limitations—to well below it, enabling complete interaction between the antioxidant and the DPPH radical.

*DPPH-based radical scavenging:* Antioxidant action data was taken in UV SPM (SHIMADZU, No. JH/FP/CIF/SP-04). Standard and test solutions (40 µL each) were transferred into separate test tubes, and 4 mL of dilute DPPH solution was added to each tube. This was agitated and incubated at 37.01 °C for 1/2 hrs. Now each sample was scanned for absorbance recorded at *517 nm*. (25)

### 2.2.5. In Silico Molecular Docking Evaluation

Computational studies were conducted using Maestro 10.5 (Schrodinger Inc., USA) on a system with an Intel® Core™ i3-2400 CPU (2.40 GHz). The crystalline str of the receptor tyrosine kinase was retrieved using PDB ID 3W2S. That was thus prepared in three steps, i.e." preprocess, optimize and minimize by protein making wizard. H2O that was altering the result by interacting to receptor, previously deleted, hydrogen atoms for needed were added. The structural free energy was optimized side by side reduced to minimum for this and force field OPLS 2005 was applied. A grid box receptor used for docking the ligands. It was found by receptor grid production program. The ligands previously prepared were docked into the generated grid using XP manner. The docking scores were the analysis criteria.

#### 2.2.5.1. Ligand–Receptor Binding Free Energetics:

The BE of ligands were noted by ΔG binding (MM-GBSA). The same software by the software Maestro 10.5 (Schrodinger Inc., USA) used. The results of the docking were raw data for above calculation. Binding energy explains types of interactions. The negative of free energy value of binding proportionate to the stability.

### 2.2.6. Prediction of ADME properties

QikProp of Schrodinger, and Maestro used for it. ADME parameters calculated by using ligPrep out as the raw for QikProp. These were evaluated, including QPlogKp (skin permeability), QPlogBB (CNS penetration), and QPlogKhsa (binding affinity to human albumin in serum). Additionally, QPPcaco and QPPMDCK values were examined to assess intestinal and cellular permeability, respectively.

## 3. Findings and Discussions

### 3.1. Chemistry

Isatin derivatives were synthesized in one-step reactions of compounds (SA01, SA02 and SA03) from Phenylsulfonyl chloride derivatives (1 mmol) and 5-bromoisatin (1 mmol). The synthesized isatin derivatives were structurally characterised by spectral methods, including FT-IR, $^{1}$H NMR, and Mass spectroscopy. Their antimicrobial action was also assessed in *in vitro*.

### 3.1.1. Analytical Data

5-bromo-1-((4-chlorophenyl)sulfonyl) indoline-2,3-dione (SA01): Red color, yield: 97%, m.p. 190-191 ºC; $^{1}$H NMR (600 MHz, DMSO-*d*$_6$) δ (ppm): 7.94 (d, *J* = 7.2 Hz, 2H, Ar-H), 7.82 (d, *J* = 7.1 Hz, 2H, Ar-H), 7.65 (d, *J* = 7.6 Hz, 2H, Ar-H), 7.56 (s, 1H, Ar-H) $^{13}$C NMR (151 MHz, DMSO-*d*$_6$) δ (ppm): 186.24 (C=O), 183.97 (C=O), 154.52, 148.79, 134.91, 134.69, 131.72 (2C), 130.72, 129.38 (2C), 123.77, 113.27, 111.64. Mass (m/z): Calculated for $C_{14}H_7BrClNO_4S$: 398.90; was found to be 398.45; Elemental analysis for $C_{14}H_7BrClNO_4S$

calculated C, 41.97; H, 1.76; N, 3.50; Found: C, 41.87; H, 1.66; N, 3.43.

5-bromo-1-((4-bromophenyl)sulfonyl) indoline-2,3-dione (SA02): Dark brownish color, yield: 98%, m.p. 198-199 °C; $^1$H NMR (600 MHz, DMSO-*d*$_6$) δ (ppm): 8.12 (d, *J* = 7.1 Hz, 2H, Ar-H), 7.90 (d, *J* = 7.4 Hz, 2H, Ar-H), 7.53 (d, *J* = 7.6 Hz, 2H, Ar-H), 7.46 (s, 1H, Ar-H). $^{13}$C NMR (151 MHz, DMSO-*d*$_6$) δ (ppm): 185.80 (C=O), 185.78 (C=O), 154.75, 135.46, 135.44, 135.37, 135.36 (2C), 135.30, 135.28, 128.35, 126.34, 113.27 (2C). Mass (m/z): Calculated for $C_{14}H_7Br_2ClNO_4S$: was found to be 445.08; Elemental analysis for $C_{14}H_7Br_2NO_4S$; calculated C, 37.78; H, 1.59; N, 3.15, Found: C, 37.63; H, 1.48; N, 3.11.

5-bromo-1-((4-fluorophenyl)sulfonyl) indoline-2,3-dione (SA03)*:* Redish color, yield: 95%, m.p. 195-197 °C; $^1$H NMR (600 MHz, DMSO-*d*$_6$) δ (ppm): 8.05 (d, *J* = 7.3 Hz, 2H, Ar-H), 7.91 (d, *J* = 7.6 Hz, 2H, Ar-H), 7.66 (d, *J* = 7.5 Hz, 2H, Ar-H), 7.45 (s, 1H, Ar-H). $^{13}$C NMR (151 MHz, DMSO-*d*$_6$) δ (ppm): 187.72 (C=O), 186.23 (C=O), 154.53, 140.54, 135.01, 132.31 (2C), 131.74, 130.97 (2C), 125.70, 123.78, 113.24, 113.22, Mass (m/z): Calculated for $C_{14}H_7BrFNO_4S$: was found to be 384.18; Elemental analysis for $C_{14}H_7BrFNO_4S$; calculated C, 43.77; H, 1.84; N, 3.65, Found: C, 43.64; H, 1.76; N, 3.59.

**Table 1. MIC (µg/ml) of the compound and standard drugs.**

| Sample | MIC Gram (+)ve bacteria | | MIC Gram (-)ve bacteria | |
|---|---|---|---|---|
| | ***Staphylococcus aureus*** | ***Bacillus subtilis*** | ***Pseudomonas putida*** | ***Escherichia coli*** |
| SA01 | 5.12 | 6.24 | 4.12 | 6.14 |
| SA02 | 5.74 | 3.12 | 6.14 | 5.79 |
| SA03 | 4.98 | 7.14 | 5.87 | 5.74 |
| Amoxicillin | 2.14 | 2.58 | 0.97 | 0.56 |
| Ciprofloxacin | 0.89 | 0.90 | 1.27 | 1.45 |

In the table (1) it is seen as expected, the standard antibiotics amoxicillin and ciprofloxacin exhibited significantly lower MIC values across all tested strains, indicating superior antibacterial efficacy compared to the synthesized compounds. Overall, the results suggest that the sulfonyl indoline-2,3-dione derivatives possess broad-spectrum antibacterial activity, though with lower potency than the reference drugs, and may serve as promising lead molecules for further structural optimization.

### 3.2. Pharmacology

#### 3.2.1. Antibacterial Activity

Two Gram positive and two Gram negative bacteria were used for this study, from MTCC (Microbial Type Culture Collection).

#### 3.2.2 Growth Inhibition Zone Assay

The antibacterial effect of the synthesized compounds was seen over four bacterial strains, namely *S. aureus* (MTCC 1192), *B. subtilis* (MTCC 1427), *E. coli* (MTCC 96), and *P. putida* (MTCC 1679), Table 1. Among the tested derivatives, SA01 exhibited MIC ranges between 4.12-6.24 µg/mL. Similarly, SA02 showed antibacterial MIC values between 3.12 and 6.14 µg/mL, while SA03 displayed MIC values from 4.98 to 7.14 µg/mL. In comparison, the standard antibiotics demonstrated higher potency, with amoxicillin exhibiting MIC values in the range of 0.56–2.58 µg/mL, and ciprofloxacin showing MIC values between 0.89 and 1.45 µg/mL.

#### 3.2.3. *In vitro* antioxidant Profiling of the Test Samples

All the newly synthesized, SA01, SA02 and SA03, applied over the DPPH free radical scavenging assay by method of *Azhar et al.,* little modifications done. Two compounds, SA02 and SA03, showed significant antioxidant activities (Figure 3). Antioxidant activity-$EC_{50}$ of SA02 is near to standard antioxidant (Table 2). DPPH assay was a dose-dependent, seen at the range (10-100 µM) dills. At a concentration of 100 µM, SA02 and SA03 showed 66.96%, and 54.81% inhibition respectively, as compared to ascorbic acid, which showed 70.77% inhibition. Compound SA02, which carries a bromo (–Br) substituent at the para position of the phenyl ring, exhibited the strongest free radical scavenging activity among the Isatin derivatives, showing a performance nearly comparable to the standard antioxidant L-ascorbic acid.

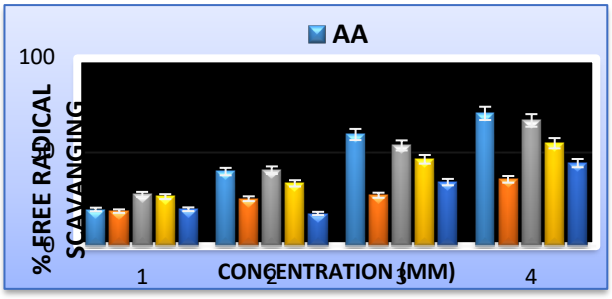


**Figure 3. Antioxidant activity displayed by compounds (SA01-03) and ciprofloxacin compared to Ascorbic acid.**

**Table 2: DPPH assay of the synthesized compounds (SA01–SA03) expressed as $EC_{50}$ values (µM), showing the influence of para-halogen substitution (Cl, Br, F) on antioxidant potential, in comparison with ciprofloxacin and the standard L-AA.**

| Compounds | R | (DPPH) $EC_{50}$ (µM) ± S.D |
|---|---|---|
| SA01 | 4-Cl | >200 |
| SA02 | 4-Br | 41.28 |
| SA03 | 4-F | 76.85 |
| ciprofloxacin | | 143.57 |
| L-AA (standard) | | 35.62 ± 0.25 |

$EC_{50}$: Concentration reducing radicals by 50%, expressed as mean ± SD, using L-AA as standard.

#### 3.2.4. Molecular docking

Docking scores, binding dynamisms, and interaction profiles of compounds are summarized (Table 3).

**Table 3. Molecular docking results of the synthesized compounds (SA01–SA03) and the reference drug ciprofloxacin, showing docking scores and predicted binding free energies (kcal/mol), indicative of their binding affinity and interaction strength with the target protein.**

| Compounds | Docking Score | Binding free energy (kcal/mol) |
|---|---|---|
| SA01 | 7.068 | -38.8 |
| SA02 | 7.918 | -44.66 |
| SA03 | 7.257 | -43.45 |
| Ciprofloxacin | 7.152 | -41.52 |

Compounds SA02 and SA03 showed high docking scores, -7.918 and -7.257, respectively, in the active main pocket of the DHFR complex contrasted to Ciprofloxacin (-7.152). It was noticed that the compound SA02 and SA03 forms only one crucial hydrogen bond with the amino acid Ala 7, whereas ciprofloxacin also forms one H-bond with the amino acid Asp 27.

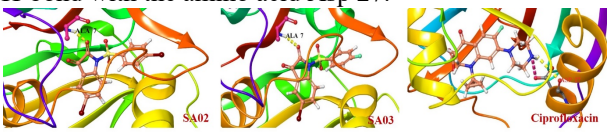


The 3D binding poses of compounds SA02, SA03, and Ciprofloxacin are shown in Figure 4. In these representations, dotted lines (yellow) show H-bonds, dotted lines (sky-blue) show π–π stacking contacts, and the atom colors are depicted as follows: carbon in reddish brown, nitrogen in blue, hydrogen in white, and oxygen in red.

**Figure 4: 3D dock pose of compound SA02, SA03, and Ciprofloxacin.**

The overlapping pattern of compounds, **SA02 and SA03,** with standard Ciprofloxacin. It has been noticed that all three compounds overlap well with each other, as represented in **Figure 5**.

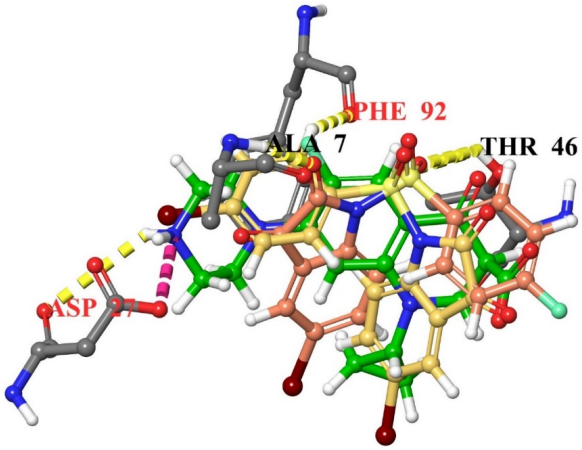


**Figure 5: Superimposition of compound SA02 (Yellowish), Ciprofloxacin (green) and SA03 (Reddish-brown).**

The two-dimensional pose of the most potent compound SA02 is shown in Figure 6. 2D view of SA02 clarified that it forms a hydro-phobic contact with Val 6, Ala 7, Ile 14, Phe 16, Ile 20, Ile 50, Val 31, Phe 98, Phe 92 and Leu 28. Aromatic ring and its attached chain also engage in weak van der Waals contacts with the non-polar side-chain region of Leu54. The polar contact also takes with amino acid Gln 95, Thr 121, Asn 18, Gln 19, Thr 46 and Ser 49. The negative charge interaction exhibited by SA02 with the amino acid Asp 27. SA02 also forms only three Glycin interactions with the amino acids Gly 93, Gly 94 and Gly 15.

The two-dimensional pose of the most potent compound, Ciprofloxacin, is shown in Figure 6. 2D view of Ciprofloxacin clarified that it forms a hydrophobic interaction occur with Phe 92, Leu 5, Val 6, Ala 7, Leu 28, Val 31, Ile 50, Trp 22, Leu 20 and Ile 14. The aromatic ring and its side chain also establish weakly forces van der Waals with the Phe98. The polar contacts involve Gln 19, Thr 121, Asn 18, Thr 46, Thr 111 and Ser 49. The negative charge interaction exhibited by Ciprofloxacin with the amino acid Asp 27. Ciprofloxacin also forms only three Glycine contacts with Gly 15, Gly 93, and Gly 94. Surface poses of both potent compound SA02 and standard Ciprofloxacin are represented in Figure 7. The surface view of SA02 demonstrates complete fitting within the enzyme's active site, similar to the positive control Ciprofloxacin.

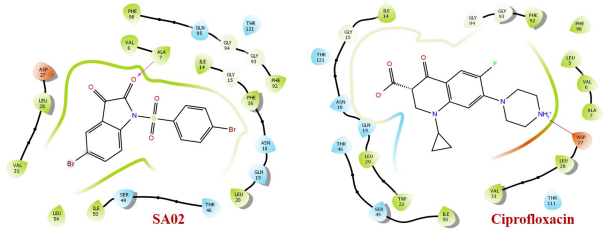


**Figure 6: 2D dock pose of compound SA02 and Ciprofloxacin.**

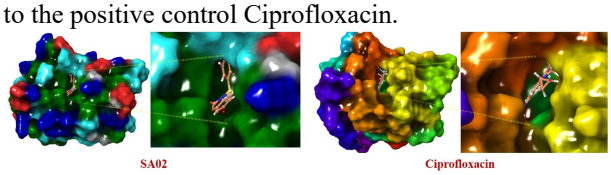


**Figure 7: Surface views of potent compound SA02 and showing that the compounds fully occupy the enzyme's active site**

Figures 8 illustrate the XP visualisation of potent compounds SA02, SA03 and standard Ciprofloxacin. In this depiction, we employed a ball-and-stick approach (green) to depict the *hydrophobic enclosure* of compounds SA02 and standard Ciprofloxacin, as well as the hydrophobic remnants (amino acid) shown in the turquoise CPK. SA02 shows one hydrogen bond with *Thr 46,* which is exactly similar to standard Ciprofloxacin. The hydrophobic part of SA02 is surrounded by Leu 20, Leu 28, Trp 22, Ile 14, Leu 5, Val 21, Val 6, and Phe 98. SA02 also shows one hydrogen bond with *Thr 46,* similar to Ciprofloxacin.

These hydrophobic interactions provided optimum lipophilicity to the synthesised compounds to cross the blood-brain barrier-like membrane, which led to better interaction with the receptor pocket of VEGFR-2 and hence better activity.

In this depiction, XP visualisation of the hydrophobically packed hydrogen bonds of potent compound SA03, we employed a ball-and-stick approach (green) to depict the hydrophobically packed hydrogen bonds of compounds SA03, which shows two hydrogen bonds with *Thr* 46 and Ala 7, with the shortest hydrogen bond length being 2.0431. The hydrophobic part of SA03 is surrounded by Leu 20, Trp 22, Ala 7, Val 6, and Phe 98. The compound SA02 and standard Ciprofloxacin do not show hydrophobically packed hydrogen bonds.

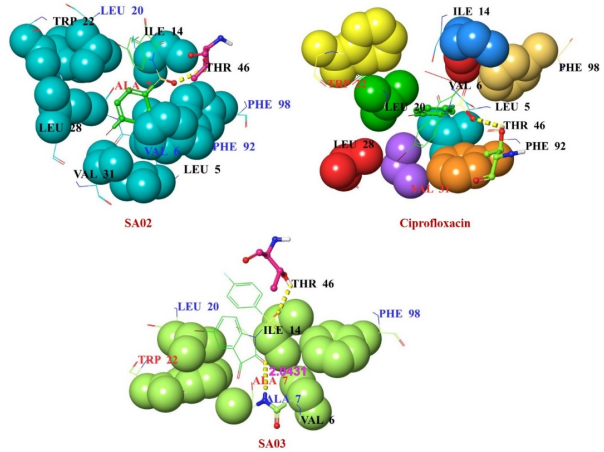


**Figure 8: XP visualisation of hydrophobic enclosures of the compounds SA02, SA03 and ciprofloxacin.**

### 3.2.5. MM-GBSA binding free energy

Table 4 indicated that the potent compounds **SA02** and SA03 fit into the DHFR receptor complex (PDB: 2W9H). The compounds, SA02 and SA03, exhibit higher docking scores and also show higher binding energy. The Binding energies of both compounds are in the range of -44.66 and -38.8 kcal/mol, respectively. Out of all, compounds SA02 and SA03 (-44.66 and -43.45) showed higher DG binding to the standard drug Ciprofloxacin (-41.52).

**Table 5. ADME of the potent compounds SA02 and Standard Ciprofloxacin**

| **Compounds** | **SA02** | **Ciprofloxacin** |
|---|---|---|
| Mol. weight | 445.08 | 333.362 |
| dipole | 7.925 | 7.76 |
| H-bond donor | 0 | 1 |
| H-bond acceptor | 7 | 4.5 |
| QPpolrz | 32.12 | 35.08 |
| QPlogPC16 | 10.72 | 9.30 |
| QPlogPoct | 16.16 | 17.4 |
| QplogPo/w | 1.66 | 10.22 |
| QPlogS | -3.15 | **-3.92** |

All the compounds are predicted to have excellent as well as acceptable QPPcaco, QPP MDCK, QPlogKP, Percent human Oral Absorption, QPlogBB, QPlogKhsa, and QPlogPo/w values. Potent compounds SA02 and standard Ciprofloxacin of this series have an acceptable range of different parameters like molecular weight, HB donor, HB acceptor, QPlogPo/w, QPlogS, QPPcaco, and they satisfy Lipinski's rule of Five. (Table 5). Similarly, Potent compounds SA02 have an acceptable range of

### 3.2.6 Prediction of ADME properties

ADME properties of potent best-docked ligand molecules are presented in Table 5, such as QPlogKP for the permeability of the skin, QPlogBB represents overall CNS activity, QPlogKhsa represents the binding of human serum albumin, QPPcaco, and QPP MDCK represent cell permeability (MDCK cells represent permeability to mimic the blood-brain barrier), etc.

| | | |
|---|---|---|
| ClQPlogS | -6.17 | -2.73 |
| QPlogHERG | -4.90 | -3.175 |
| QPPcaco | 244.28 | 17.31 |
| QplogBB(-3 to 1.2) | -0.72 | -0.54 |
| QPP MDCK | 761.865 | 13.84 |
| QPlogKp | -3.69 | -6.34 |
| QPlogKhsa | -0.62 | 0.022 |
| Percent of Human Oral | 79.45 | 50.98 |
| Rule of three | 0 | 1 |
| Rule of five | 0 | 0 |

QPlogS, QPPcaco, and Primary Metabolites, and hence they satisfy Lipinski's rule of three, but QPPcaco of standard ciprofloxacin are not in an acceptable range (17.31). At last, compound SA02 has good oral absorption, QPP MDCK, and QPPcaco as their values are in an acceptable range: 79.45%, 761.86, 244.28, respectively. Unlike the SA02, ciprofloxacin has a below-par value of oral absorption, QPP MDCK, QPPcaco(50.98, 13.84, 17.31, respectively). Out of all,

compound SA02 displayed the best ADME profile, and hence good pharmacokinetics and pharmacodynamics properties.

**4. Discussion**

The present study defines the synthesis, structural elucidation and antibacterial evaluation of three novel isatin derivatives (SA01–SA03) prepared by the reaction of 5-bromoisatin with phenylsulfonyl chloride derivatives in a one-step procedure. The synthetic strategy was found to be straightforward, yielding compounds in high purity with excellent yields (95–98%) (24). The observed color differences (red for SA01 and SA03, dark brownish for SA02) can be attributed to variations in the electronic environment of the sulfonyl-substituted phenyl ring, which slightly alters the conjugation across the isatin scaffold (26, 27).

All compounds were fully characterized by $^{1}$H NMR, $^{13}$C NMR and mass spectrometry. The proton NMR spectra of the derivatives displayed characteristic downfield aromatic signals between δ 7.4–8.1 ppm, corresponding to the isatin ring protons and the para-substituted phenyl sulfonyl groups (28). In particular, SA01 exhibited distinct doublets at δ 7.94 and δ 7.82 ppm, consistent with a 4-chlorophenyl sulfonyl substitution. Similarly, SA02 and SA03 showed well-resolved doublets in the same region, indicative of symmetric para-substitution on the phenyl ring. The singlet around δ 7.45–7.56 ppm corresponded to the alone isatin aromatic proton, which further confirmed substitution at the nitrogen atom.

The $^{13}$C NMR spectra supported the proposed structures by showing two strong carbonyl resonances (δ 183–187 ppm) attributed to C-2 and C-3 of the isatin nucleus. Additionally, downfield signals at δ 148–155 ppm confirmed the presence of deshielded aromatic carbons adjacent to the electron-withdrawing sulfonyl substituents. The mass spectra of all three derivatives revealed molecular ion peaks that were in close agreement with the calculated m/z values, further validating successful synthesis (29).

The antibacterial action of the synthesized derivatives was assessed on Gram +ve strains (S. aureus, B. subtilis) and two Gram -ve strains (E. coli, P. putida). All three derivatives exhibited moderate inhibitory effects, with MIC range lies in 3.12 to 7.14 µg/mL.

Interestingly, the halogen substitution on the phenylsulfonyl moiety significantly influenced the antibacterial potency (30, 31)**.** The bromo-substituted derivative (SA02) demonstrated the most potent activity (MIC 3.12–6.14 µg/mL), followed by the chloro derivative (SA01; MIC 4.12–6.24 µg/mL), whereas the fluoro derivative (SA03) showed relatively weaker inhibition (MIC 4.98–7.14 µg/mL). This trend may be rationalized by considering the electronic and steric effects of halogen substituents: bromine, being bulkier and less electronegative, could enhance lipophilicity and promote stronger interactions with bacterial membrane components, thereby improving permeability and antibacterial activity. In contrast, the fluoro group, despite its strong electronegativity, may limit lipophilic interactions and result in reduced potency (32, 33).

When compared to standard antibiotics, the synthesized compounds displayed lower activity (amoxicillin MIC: 0.56–2.58 µg/mL; ciprofloxacin MIC: 0.89–1.45 µg/mL). However, the derivatives still exhibited promising antibacterial potential, particularly considering their simple one-step synthesis, novel substitution pattern, and activity in the low µg/mL range. This finding is noteworthy, as sulfonyl-isatin hybrids are relatively unexplored, and structural modifications may further optimize their efficacy.

The results suggest that substitution on the phenylsulfonyl group plays a critical role in modulating antibacterial activity:

- SA02 (4-bromo substitution) → highest activity, likely due to enhanced lipophilicity and membrane penetration.
- SA01 (4-chloro substitution) → intermediate activity, balancing steric bulk and electronic effects.
- SA03 (4-fluoro substitution) → lowest activity, possibly due to lower hydrophobic interactions and altered binding affinity.

Additionally, the presence of the 5-bromo substituent on the isatin core may further contribute to activity by enhancing electron delocalization and facilitating halogen–π or halogen bonding interactions with bacterial enzyme targets (34).

The observed antibacterial activity of SA01–SA03 indicates that isatin–sulfonyl hybrids represent a promising scaffold for developing new antimicrobial agents.

**5. Limitations and Future Directions**

Despite these positive findings, certain limitations should be acknowledged. First, the proposed antibacterial mechanism of action is primarily supported by in silico docking and binding free energy analysis targeting bacterial dihydrofolate reductase (DHFR). While these computational results provide valuable mechanistic insights, they remain predictive in nature. Experimental validation through enzyme inhibition assays or target-specific biochemical studies will be essential to conclusively confirm the involvement of DHFR or alternative molecular targets.

Second, the biological evaluation was limited to in vitro antibacterial susceptibility testing using MIC determination and zone of inhibition assays. Although these assays establish antibacterial potency, they do not differentiate between bacteriostatic and bactericidal effects, nor do they capture time-dependent killing kinetics. Future studies incorporating time–kill assays, post-antibiotic effect analysis, and resistance development profiling would deliver a more complete thoughtful of the antibacterial behavior of these compounds.

Third, cytotoxicity and selectivity assessments against mammalian cell lines were not performed in the current work. Such studies are crucial to establish therapeutic safety margins and to determine selectivity indices, which are key parameters for advancing lead compounds toward preclinical development. Incorporation of in vitro

cytotoxicity assays and hemolytic studies will therefore be an important next step.

Although antioxidant activity was evaluated to explore the broader pharmacological relevance of the scaffold, the direct contribution of this property to antibacterial efficacy was not experimentally investigated. Future work may focus on elucidating whether the antioxidant potential of these compounds confers additional therapeutic benefits, particularly in infection models associated with oxidative stress and inflammatory damage.

Finally, while in silico ADME predictions indicated favorable drug-like properties—especially for the lead compound SA02—these findings require experimental validation. Pharmacokinetic studies, metabolic stability assessments, and in vivo efficacy evaluations in suitable infection models will be necessary to confirm the translational potential of these sulfonyl-linked 5-bromoisatin derivatives.

In future research, systematic structural optimization of the lead scaffold, including exploration of alternative substitutions on both the isatin core and the sulfonyl phenyl ring, may further enhance antibacterial potency and selectivity. Collectively, addressing these limitations will strengthen the mechanistic understanding and accelerate the progression of these compounds toward viable antibacterial drug candidates.

## 6. Conclusion

We successfully designed, synthesized, and biologically evaluated a new series of sulfonyl-linked 5-bromoisatin derivatives (SA01–SA03) as potential antibacterial agents. The compounds were obtained via a straightforward one-step reaction with excellent yields (95–98%), highlighting the synthetic feasibility and scalability of the approach. Structural elucidation using ^1H NMR, ^13C NMR and mass spectrometry unequivocally confirmed the successful incorporation of para-halogen–substituted phenylsulfonyl moieties onto the isatin nucleus, validating the intended molecular design

Biological evaluation revealed that all synthesized derivatives possess antibacterial activity on Gram +ve (*S. aureus*, *B. subtilis*) and Gram -ve (*E. coli*, *P. putida*) strains, with MIC values in the low micromolar range. Among the series, the 4-bromo–substituted analogue SA02 consistently appeared as the strongest compound, exhibiting MIC ranges of 3.12–6.14 µg/mL. Although the antibacterial efficacy of the synthesized compounds was lower than that of standard antibiotics such as amoxicillin and ciprofloxacin, their activity compares favorably with many previously reported isatin derivatives, underscoring the value of sulfonyl-isatin hybridization as a drug design strategy.

Structure–Activity Relationship (SAR) analysis clearly indicates that para-halogen substitution on the phenylsulfonyl ring plays a decisive role in modifying biological activity. The superior performance of SA02 suggests that the larger and more polarizable bromine atom enhances lipophilicity, membrane permeability, and intermolecular interactions with bacterial targets, whereas the fluoro analogue (SA03) showed comparatively weaker activity. This SAR trend was consistently supported by in vitro antibacterial results, antioxidant profiling, and in silico studies.

The antioxidant evaluation further differentiated the compounds, with SA02 again displaying the most promising activity ($EC_{50}$ = 41.28 µM), approaching that of the standard antioxidant L-ascorbic acid. This dual antibacterial–antioxidant behavior enhances the pharmacological relevance of the scaffold and suggests potential added therapeutic benefits, particularly in infection-associated oxidative stress.

Molecular docking and MM-GBSA binding free energy analyses provided strong mechanistic support for the experimental findings. SA02 and SA03 demonstrated higher docking scores and more favorable binding free energies than ciprofloxacin, indicating stable and energetically favorable interactions within the DHFR active site. The close overlap of SA02 with ciprofloxacin in the binding pocket, along with comparable hydrogen bonding and hydrophobic interaction profiles, rationalizes the observed antibacterial activity at the molecular level. Importantly, the predicted ADME properties of SA02 were within acceptable ranges, with superior oral absorption, permeability, and pharmacokinetic parameters compared to ciprofloxacin, further strengthening its profile as a lead compound.

In conclusion, this work establishes sulfonyl-linked 5-bromoisatin derivatives—particularly the 4-bromo analogue SA02—as promising lead scaffolds for antibacterial drug development. The convergence of efficient synthesis, consistent in vitro activity, supportive in silico evidence, favorable ADME predictions, and preliminary antioxidant potential positions SA02 as a strong candidate for further optimization. Future studies focusing on structural refinement, target validation, toxicity profiling, and in vivo efficacy are warranted to advance these compounds toward preclinical development.

## 6. References


1. Salam, M. A., Al-Amin, M. Y., Salam, M. T., Pawar, J. S., Akhter, N., Rabaan, A. A., & Alqumber, M. A. (2023, July). Antimicrobial resistance: a growing serious threat for global public health. In *Healthcare* (Vol. 11, No. 13, p. 1946). MDPI.
2. Nazir, A., Nazir, A., Zuhair, V., Aman, S., Sadiq, S. U. R., Hasan, A. H., & Bulimbe, D. B. (2025). The Global Challenge of Antimicrobial Resistance: Mechanisms, Case Studies, and Mitigation Approaches. *Health Science Reports*, *8*(7), e71077.
3. Kaur, T., Bose, D., Bhattacharya, R., & Biju, M. (2025). Microbiome-Mediated Disease Suppression: A Promising Avenue for Phytophthora Management in Commercial Crops Using Phytochemicals Obtained from Medicinal Plants. *Industrial Biotechnology*, *21*(3), 157-179.
4. Nath, P., Mukherjee, A., Mukherjee, S., Banerjee, S., Das, S., & Banerjee, S. (2021). Isatin: a scaffold with immense biodiversity. *Mini Reviews in Medicinal Chemistry*, *21*(9), 1096-1112.

5. Guo, H. (2019). Isatin derivatives and their anti-bacterial activities. *European Journal of Medicinal Chemistry*, *164*, 678-688.
6. Song, F., Li, Z., Bian, Y., Huo, X., Fang, J., Shao, L., & Zhou, M. (2020). Indole/isatin-containing hybrids as potential antibacterial agents. *Archiv der Pharmazie*, *353*(10), 2000143.
7. Patel, A., Bari, S., Talele, G., Patel, J., & Sarangapani, M. (2006). Synthesis and antimicrobial activity of some new isatin derivatives.
8. Andreani, A., Burnelli, S., Granaiola, M., Leoni, A., Locatelli, A., Morigi, R., ... & Greco, E. (2010). New isatin derivatives with antioxidant activity. *European journal of medicinal chemistry*, *45*(4), 1374-1378.
9. Jarapula, R., Gangarapu, K., Manda, S., & Rekulapally, S. (2016). Synthesis, in vivo anti-inflammatory activity, and molecular docking studies of new isatin derivatives. *International journal of medicinal chemistry*, *2016*(1), 2181027.
10. Xu, Z., Zhang, S., Gao, C., Fan, J., Zhao, F., Lv, Z. S., & Feng, L. S. (2017). Isatin hybrids and their anti-tuberculosis activity. *Chinese Chemical Letters*, *28*(2), 159-167.
11. Ferraz de Paiva, R. E., Vieira, E. G., Rodrigues da Silva, D., Wegermann, C. A., & Costa Ferreira, A. M. (2021). Anticancer compounds based on isatin-derivatives: Strategies to ameliorate selectivity and efficiency. *Frontiers in molecular biosciences*, *7*, 627272.
12. Phogat, P., & Singh, P. (2015). A mini review on central nervous system potential of isatin derivatives. *Central Nervous System Agents in Medicinal Chemistry (Formerly Current Medicinal Chemistry-Central Nervous System Agents)*, *15*(1), 28-31.
13. Pawar, V. S., Lokwani, D. K., Bhandari, S. V., Bothara, K. G., Chitre, T. S., Devale, T. L., ... & Parikh, J. K. (2011). Design, docking study and ADME prediction of Isatin derivatives as anti-HIV agents. *Medicinal chemistry research*, *20*(3), 370-380.
14. Al-Mudhafar, M. M. J., & Wadi, J. S. (2024). Synthesis and biological activity evaluation of new isatin-gallate hybrids as antioxidant and anticancer agents (in vitro) and in silico study as anticancer agents and coronavirus inhibitors.
15. El-Miligy, M. M., Rida, S. M., Ashour, F. A., Badr, M. H., El-Bassiony, E. M., El-Demellawy, M. A., & Omar, A. M. (2018). Dual inhibitors of hepatitis C virus and hepatocellular carcinoma: design, synthesis and docking studies. *Future Science OA*, *4*(1), FSO252.
16. Cheke, R. S., Patil, V. M., Firke, S. D., Ambhore, J. P., Ansari, I. A., Patel, H. M., ... & Snoussi, M. (2022). Therapeutic outcomes of isatin and its derivatives against multiple diseases: recent developments in drug discovery. *Pharmaceuticals*, *15*(3), 272.
17. Nath, P., Mukherjee, A., Mukherjee, S., Banerjee, S., Das, S., & Banerjee, S. (2021). Isatin: a scaffold with immense biodiversity. *Mini Reviews in Medicinal Chemistry*, *21*(9), 1096-1112.
18. Ovung, A., & Bhattacharyya, J. (2021). Sulfonamide drugs: structure, antibacterial property, toxicity, and biophysical interactions. *Biophysical reviews*, *13*(2), 259-272.
19. Sarker, A., Hossain, T., Bashir, M. N., Fatema, K. J., & Rahman, A. K. M. L. (2019). Synthesis and characterization of N, N′-bis (isatin) diamino zirconium (IV) complexes. *Bangladesh Journal of Scientific and Industrial Research*, *54*(4), 297-306.
20. Rahman, A. K. M. L., Sarker, A., Bashir, M. N., & Hossain, M. L. (2023). Molybdenum (VI) complexes of N, N′-bis isatin diamine Schiff base: Synthesis and characterization. *Bangladesh Journal of Scientific and Industrial Research*, *58*(4), 201-208.
21. Shaldam, M. A., Almahli, H., Angeli, A., Badi, R. M., Khaleel, E. F., Zain-Alabdeen, A. I., ... & Tawfik, H. O. (2023). Discovery of sulfonamide-tethered isatin derivatives as novel anticancer agents and VEGFR-2 inhibitors. *Journal of Enzyme Inhibition and Medicinal Chemistry*, *38*(1), 2203389.
22. Salam, M. A., Al-Amin, M. Y., Pawar, J. S., Akhter, N., & Lucy, I. B. (2023). Conventional methods and future trends in antimicrobial susceptibility testing. *Saudi journal of biological sciences*, *30*(3), 103582.
23. Chowdhary, S., Shalini, Arora, A., & Kumar, V. (2022). A mini review on isatin, an anticancer scaffold with potential activities against neglected tropical diseases (NTDs). *Pharmaceuticals*, *15*(5), 536.
24. Shu, V. A., Eni, D. B., & Ntie-Kang, F. (2025). A survey of isatin hybrids and their biological properties. *Molecular diversity*, *29*(2), 1737-1760.
25. Iqbal, M. A., Husain, A., Alam, O., Khan, S. A., Ahmad, A., Haider, M. R., & Alam, M. A. (2020). Design, synthesis, and biological evaluation of imidazopyridine-linked thiazolidinone as potential anticancer agents. *Archiv der Pharmazie*, *353*(10), 2000071.
26. Chowdhary, S., Shalini, Arora, A., & Kumar, V. (2022). A mini review on isatin, an anticancer scaffold with potential activities against neglected tropical diseases (NTDs). *Pharmaceuticals*, *15*(5), 536.
27. Liu, W., Zhu, H. M., Niu, G. J., Shi, E. Z., Chen, J., Sun, B., ... & Yang, C. (2014). Synthesis, modification and docking studies of 5-sulfonyl isatin derivatives as SARS-CoV 3C-like protease inhibitors. Bioorganic & medicinal chemistry, 22(1), 292-302.
28. Liu, W., Zhu, H. M., Niu, G. J., Shi, E. Z., Chen, J., Sun, B., ... & Yang, C. (2014). Synthesis, modification and docking studies of 5-sulfonyl isatin derivatives as SARS-CoV 3C-like protease

inhibitors. *Bioorganic & medicinal chemistry*, *22*(1), 292-302.
29. Guo, H. (2019). Isatin derivatives and their anti-bacterial activities. *European Journal of Medicinal Chemistry*, *164*, 678-688.
30. Song, F., Li, Z., Bian, Y., Huo, X., Fang, J., Shao, L., & Zhou, M. (2020). Indole/isatin-containing hybrids as potential antibacterial agents. *Archiv der Pharmazie*, *353*(10), 2000143.
31. Altamimi, M., Syed, S. A., Tuzun, B., Alhazani, M. R., Alnemer, O., & Bari, A. (2024). Synthesis, biological evaluation and molecular docking of isatin hybrids as anti-cancer and anti-microbial agents. *Journal of enzyme inhibition and medicinal chemistry*, *39*(1), 2288548.
32. Cheke, R. S., Patil, V. M., Firke, S. D., Ambhore, J. P., Ansari, I. A., Patel, H. M., ... & Snoussi, M. (2022). Therapeutic outcomes of isatin and its derivatives against multiple diseases: recent developments in drug discovery. *Pharmaceuticals*, *15*(3), 272.
33. Grewal, A. S. (2014). Isatin derivatives with several biological activities. *International Journal of Pharmaceutical Research*, *6*(1), 1-7.
34. Elsaman, T., Mohamed, M. S., Eltayib, E. M., Abdel-Aziz, H. A., Abdalla, A. E., Munir, M. U., & Mohamed, M. A. (2022). Isatin derivatives as broad-spectrum antiviral agents: the current landscape. *Medicinal Chemistry Research*, *31*(2), 244-273.